Preliminary investigation of fracture transmissivity in unconventional shales as a function of CO_2 induced swelling

Johnathan Moore[2], Dustin Crandall[1], Circe Verba[1], and Christina Lopano[1]
National Energy Technology Laboratory – [1]U.S. Department of Energy, [2]AECOM

Research & Innovation Center

Background

In this study, the transmissivity evolution of fractured Bakken and Marcellus shales exposed to CO_2 were evaluated in a traditional core flow setup. Computed Tomography (CT) was used to observe bulk mechanical changes, and differential pressure was measured using single phase liquid CO_2 flows to calculate transmissivity. The samples were characterized for bulk composition using X-ray diffraction (XRD), electron microscopy, and total organic carbon (TOC) analysis. Dual beam focused ion beam scanning electron microscopy (FIB-SEM) was utilized to discern microstructural features below the resolution of the CT scans.

CT scanning revealed negligible changes in the fracture aperture and shale structure. However, flow studies confirmed a reduction in permeability, suggesting a bulk decrease in fracture aperture that could be attributed to swelling. The causes of the matrix swelling are under investigation; however, CO_2 sorption on the organic matter in the shale is the most likely cause of matrix swelling for the Bakken shale. The XRD data did not show the presence of swelling clays with the clay fraction being dominated by illite and mica. The TOC ranged from 2.3% in the Marcellus shale samples to nearly 20% in Bakken shale samples. FIB-SEM analyses showed the presence of kerogen-rich regions with varying morphologies that are nonporous, pendular, and spongy in nature; organic porosity by volume was approximately 2% and 11% in Marcellus and Bakken shales respectively.

These analyses illustrate the physical properties and responses of fractured unconventional black shales to CO_2 exposure. Future work will focus on identifying specific components that are contributing to swelling.

Marcellus Shale
-> Outcrop in Bedford, Pennsylvania
-> Well in Greene Co., Pennsylvania (~7800 ft)

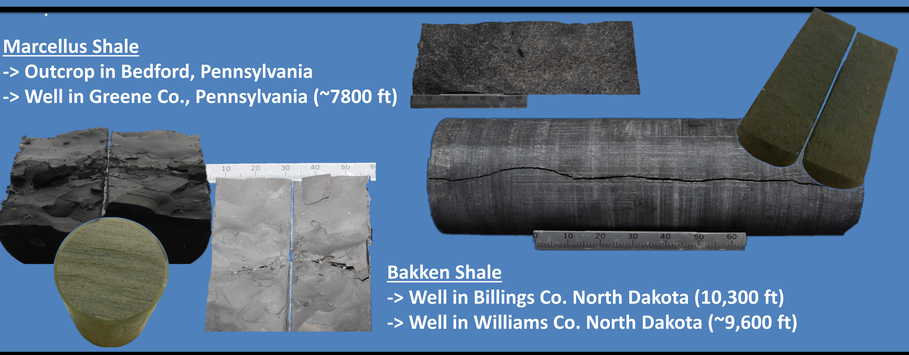

Bakken Shale
-> Well in Billings Co. North Dakota (10,300 ft)
-> Well in Williams Co. North Dakota (~9,600 ft)

Equipment and Procedures

CT with NorthStar Inc. X5000
- Resolution:
- Image Software: ImageJ [1], Northstar Inc. Efx®, and Ilastik [2]
- Data Output: 16-bit Tiff

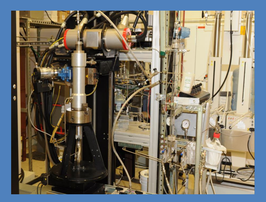

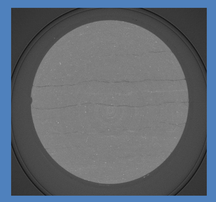

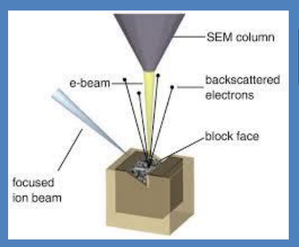

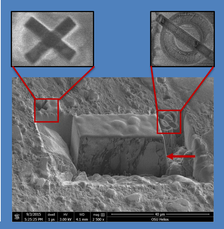

FIB-SEM with Helios 650 Ultra Resolution Dual Beam FEG
- Impregnation with epoxy & Pd coated
- Backscatter electron (BSE) taken at 5 kV
- SEM performed at (9-18) kV
- Image Software: Avizo®

Carbon totals
- Total Carbon – Perkin Elmer 2400 Series II CHNS/O Elemental Analyzer - % Weight
- Total Inorganic Carbon – Acid Digestion (% Weight)
- Total Organic Carbon = Total Carbon – Inorganic

X-Ray Diffraction with PANanalytical X'Pert Pro
- 45 kV, 40 mA with 1000s
- Compared to ICDD database
- Alcohol used to remove epoxy

Vertical Aperture (b_V)

Convert to Binary* [Ilastik, ImageJ]

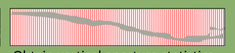

Obtain vertical aperture statistics with Python [3] scripts

Generate aperture maps based on vertical aperture

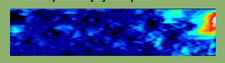

Simple method for approximating fracture geometry
***Loss of small scale heterogeneity**

Hydraulic Aperture (b_H)

Determined via Q measurements
- **Application of Darcy Law**
- **Application of simple cubic law [4]**

Note: assumes single phase laminar flow

$$b = \sqrt[3]{Q * \frac{12\mu L}{W * \Delta P}} \qquad T = Q\mu \frac{L}{\Delta P}$$

Results

X-Ray Diffraction & Total Carbon

Mineral phase	General Formula	Bakken 1	Bakken 2	Marcellus
Quartz	SiO_2	Major	Major	Major
Illite/Mica	$K(Al,Fe,Mg)_{2-3}AlSi_3O_{10}(OH)_2$	Major	Major	Minor
K-feldspar	$KAlSi_3O_8$	Minor	Minor	<Detection
Chlorite	$(Mg,Fe)_5Al(AlSi_3O_{10})(OH)_8$	Minor	Minor	<Detection
Pyrite	FeS_2	Trace	Trace	Trace
Dolomite	$CaMg(CO_3)_2$	Trace	Trace	Minor
Calcite	$CaCO_3$	Trace	Trace	Major
Carbon W% (Non-Min)	Total Carbon	21.5	21.83	11.46
	Organic Carbon	20.32	21.48	6.40
	Inorganic Carbon	1.18	0.35	5.06

Notes: Major ~ > 25%; Minor ~ 5-25%; Trace ~ < 5%.

FIB-SEM

Sample	Bakken	Marcellus
Matrix (vol)	73%	93.50%
Porosity	27%	4.12%
Organic (vol)	11%	2.32%
Organic porosity	X	3.55%

Bakken Shale Porosity Isolated

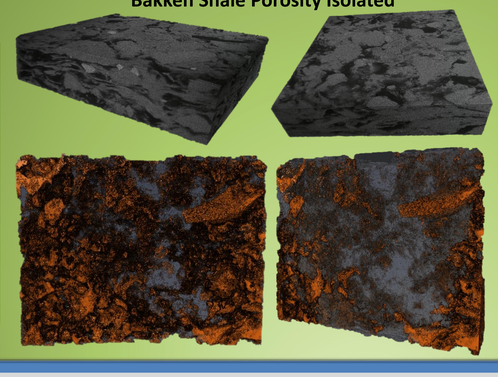

Organic Porosity Examples & Findings

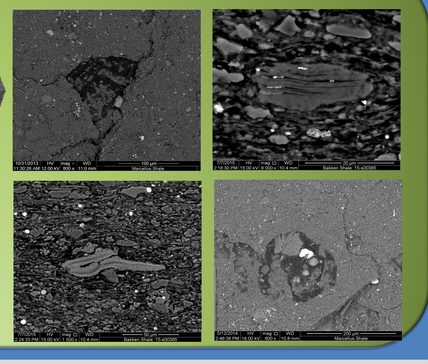

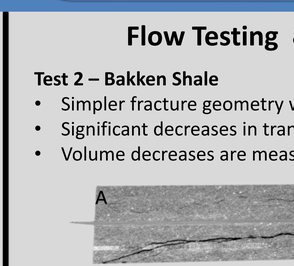

Test 1 – Bakken Shale
- Showed promise in permeability reduction
- Temporal data are lacking and scan resolution is an issue
- Complex fracture geometry & epoxy difficult to differentiate from CO_2

B

Sample Interval	Average Δb_H (μm)
16 Hour	2.19
36 Hour	2.47
118 Hour	2.18

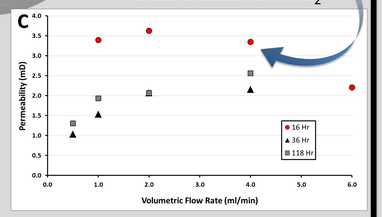

A) X/Y cross section showing fracture complexity, B) calculated hydraulic apertures based on flow data, C) permeability calculated from flow data showing temporal change.

Fig B: Each line represents 11 unique profiles drawn across the aperture image and the resulting average aperture. A gradual shift in aperture correlates with the changes in transmissivity.
**The aperture data from the 72 hour scan is an outlier and appears in other graphs presented.

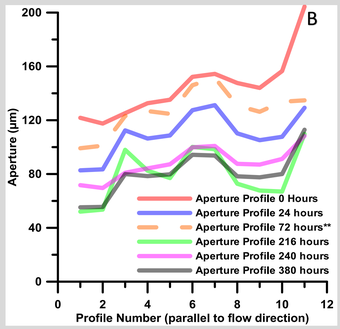

Flow Testing & CT Scanning

Test 2 – Bakken Shale
- Simpler fracture geometry with two interconnected parallel fractures
- Significant decreases in transmissivity through the experiment; non-linear changes
- Volume decreases are measureable from CT data

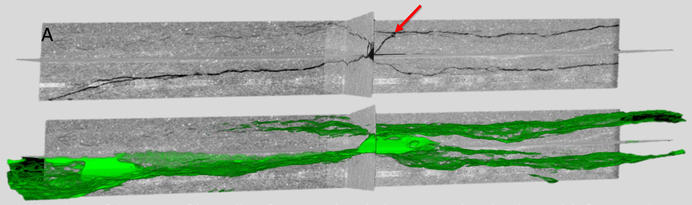

Fig A: Orthoview of 3D scan of base-line fracture the shale core and orthoview with fracture in 3D (green). Fracture plane connected by perpendicular splay (red arrow).

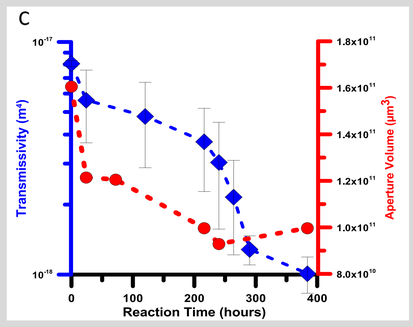

Fig C: Transmissivity and aperture volume (CT derived) plotted versus reaction time. The decrease in transmissivity corroborates well with the decrease in aperture volume. The large deviations observed within the transmissivity data are a result of some non-laminar flow rates inducing turbulence and variability.

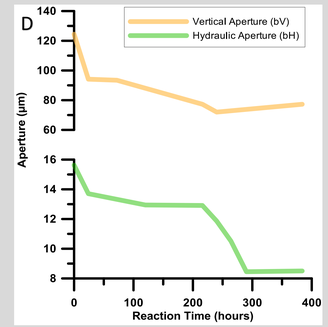

Fig D: The upper plot is the average vertical aperture derived from CT data and the lower plot is the average hydraulic aperture derived from flow data. The magnitude of difference is expected due to the inherent assumptions of plate based flow.

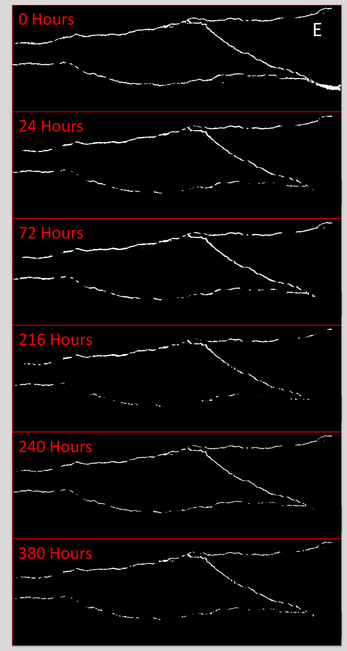

Fig E: Time series showing the middle X/Y slice of the fracture as CO_2 exposure progresses. A clear decrease in aperture can be seen from the CT scans. This is especially true within the bottom splay as it almost entirely disappears during the scan.

Test 3 – Marcellus Shale

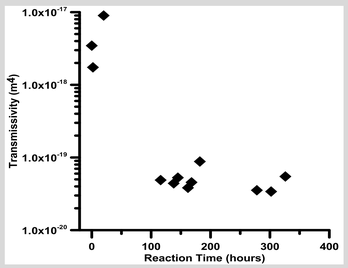

- Initial geochemistry shows greater content of carbonate and less carbon
- Inferred swelling potential, derived from flow data and initial scans, is not straight forward as in other tests
- More analysis will need to be completed with CT data and FIB-SEM

Summary
- Initial geochemistry and CT data acquired on two distinct shale types
- Data suggests swelling correlation with organic content
- Higher frequency data shows non-linear reduction in permeability

Ongoing Work
- Experiments with higher frequency flow measurements and CT scans
- Additional samples are being assessed to evaluate formation heterogeneity
- Higher frequency data shows non-linear reduction in permeability
- FIB-SEM mapping of organic porosity and potential correlation with swelling potential

Acknowledgements

The authors would like to thank Bryan Tennant, Karl Jarvis, Denny Stanko, Mengling Stuckman, and Roger Lapeer for their laboratory assistance & technical insights. Thank you to Beth Kutz and the EERC for providing geologic samples.

References:

1. Rasband, W.S. (2016) ImageJ, U. S. National Institutes of Health, Bethesda, Maryland, USA, http://imagej.nih.gov/ij/, (Accessed 2/23/2016).
2. C. Sommer, C. Straehle, U. Köthe and F. A. Hamprecht, "Ilastik: Interactive learning and segmentation toolkit," *2011 IEEE International Symposium on Biomedical Imaging: From Nano to Macro*, Chicago, IL, 2011, pp. 230-233. doi: 10.1109/ISBI.2011.5872394
3. Python Software Foundation. Python Language Reference, version 2.7. Available at http://www.python.org
4. Witherspoon, P.A., Wang, J.S.Y., Iwai, K., and Gale, J.E. (1980) Validity of Cubic Law for Fluid-Flow in a Deformable Rock Fracture, Water Resources Research, 16(6), 1016-1024.